Efficient Finite Element Analysis of Waveguides with Lossy Inhomogeneous Anisotropic Materials Characterized by Arbitrary Permittivity and Permeability Tensors

Luis Valor and Juan Zapata

Abstract—**This paper presents a new finite element formulation for solving arbitrarily shaped waveguides including lossy inhomogeneous anisotropic media. The materials are characterized by simultaneous $[\varepsilon]$ and $[\mu]$ full tensors. Complex-mode computation, spurious-mode suppression and the possibility of specifying the frequency as an input parameter are also achieved. The formulation leads to a quadratic eigenvalue problem of dimension N which is transformed into an efficient $2N$-dimensional generalized eigensystem with sparse complex matrices. This eigensystem is solved by the subspace method, taking full advantage of the sparsity of the matrices. Permittivity and permeability tensors with some null terms allow an additional reduction from the N-dimensional quadratic eigenvalue problem to a N-dimensional sparse complex generalized eigensystem. The proposed method has been validated by analyzing different lossy, inhomogeneous and anisotropic waveguides. Results show good agreement with previously published data.**

I. Introduction

RECENTLY, the dispersion characteristics of microwave and millimeter wave integrated circuits (MIC's) involving anisotropic materials as substrates and superstrates have sparked a growing interest in the field of applications for nonreciprocal devices. Technological advances enable the integration of different materials into composite MIC structures which results in nonreciprocal transmission effects. These effects are well documented for some specific MIC's [1]. Moreover, dielectric waveguides which employ anisotropic materials play an important role as fundamental components of optoelectronic and microwave devices. Consequently, some efforts have been devoted to the analysis of different transmission lines on substrates characterized by $[\varepsilon]$ and/or $[\mu]$ tensors [2]–[14].

Most of such cases involve complex transversal shapes. Because of this, they do not lend themselves to analytical solutions. The finite element method (FEM), one of the most flexible, widely used and powerful numerical methods, has become an important tool for solving these kinds of structures. In order to rigorously evaluate the propagation characteristics of lossy inhomogeneous anisotropic waveguides by means of FEM, a vectorial wave analysis is required.

Existing FEM formulations, useful for analyzing complex waveguide structures, were compared in [15] with regard to different points of view. Features that should be stressed when solving inhomogeneous anisotropic waveguides by FEM are

a) Capability of handling losses.

b) Ability to compute complex modes.

c) Possibility of solving arbitrarily shaped waveguides with reentrant corners.

d) Ability to model simultaneous dielectric and magnetic anisotropic materials.

e) Capability of handling full $[\varepsilon]$ and $[\mu]$ tensors.

f) Spurious-mode suppression.

g) Matrix-sparsity of the resulting eigensystem.

h) Possibility of specifying the frequency as input parameter and solving for the propagation constant as eigenvalue solution.

Most of the reported methods only partially fulfill these requirements. In this way, the formulation proposed by Lu *et al.* [7], [8] employs an accurate nodal element to analyze waveguides with dielectric anisotropic tensor of the form $[\varepsilon] = [\varepsilon_{tt}] + \varepsilon_{zz}\hat{z}\hat{z}$, with $[\varepsilon_{tt}]$ two-by-two symmetrical tensor. This analysis leads to a sparse eigensystem which permits to handle losses and complex modes. However, waveguides with sharp edges rend the system non-convergent. Dillon *et al.* [9] proposed a three component vector finite element formulation where the permeability tensor has the form $[\mu] = [\mu_{tt}] + \mu_{zz}\hat{z}\hat{z}$. In this case an eigenvalue problem with the phase constant as eigenvalue is obtained. In [16] Lee developed an edge-element-based method to analyze lossy inhomogeneous isotropic waveguides with sharp edges. This method leads to solving a generalized eigensystem with sparse matrices. Hayata *et al.* proposed in [10] a formulation to study lossy waveguides in which $[\varepsilon]$ may be a full tensor. Such a formulation leads to a full-matrix eigensystem.

In all these methods, the frequency is specified as input parameter and the eigensystem is solved for the propagation constant. Other methods, such as the one suggested by Bardi *et al.* in [11], solve a sparse eigensystem to obtain the frequency as the eigenvalue. This formulation can model waveguides with materials where full $[\varepsilon]$ and $[\mu]$ tensors can

Manuscript received December 8, 1994; revised June 29, 1995.

The authors are with the Grupo de Electromagnetismo Aplicado y Microondas, Departamento de Electromagnetismo y Teoría de Circuitos, Universidad Politécnica de Madrid, E.T.S.I. Telecomunicación, Ciudad Universitaria s/n, 28040 Madrid, Spain.

IEEE Log Number 9414242.

exist simultaneously. However, losses and complex modes can not be taken into account while four degrees of freedom in each nodal point are used.

In this paper, a new FEM formulation is proposed to analyze waveguides with materials where full $[\varepsilon]$ and $[\mu]$ tensors can exist simultaneously. This formulation leads to a sparse complex quadratic eigenvalue problem of dimension N (N = number of degrees of freedom) which is transformed into a $2N$-dimensional sparse complex generalized form. In particular cases where the properties of the material can be expressed as $[\varepsilon] = [\varepsilon_{tt}] + \varepsilon_{zz}\hat{z}\hat{z}$, $[\mu] = [\mu_{tt}] + \mu_{zz}\hat{z}\hat{z}$, with $[\varepsilon_{tt}]$, $[\mu_{tt}]$ two-by-two tensors, the initial quadratic eigensystem is simplified to a N-dimensional sparse complex generalized form.

In the method proposed in this paper, the frequency is specified as an input parameter and the system is solved for the complex propagation constant as eigenvalue. Therefore it is possible to handle losses and to compute complex modes.

The method employs an edge element which suppresses spurious solutions and is appropriate for solving arbitrarily shaped waveguides including reentrant corners. Numerical examples are presented to illustrate the different features of the method as quoted in a)–h). Computed results agree well with previously available data.

II. Theoretical Analysis

In this paper any material is typified, from the macroscopic point of view, by means of its characteristic bianisotropic six-by-six tensor $[M]$. This tensor is expressed as

$$[M] = \begin{bmatrix} [\varepsilon] & 0 \\ 0 & [\mu] \end{bmatrix}$$

where $[\varepsilon] = \varepsilon_0\overline{\varepsilon}$ and $[\mu] = \mu_0\overline{\mu}$ represent the permittivity and the permeability, respectively, ε_o and μ_o are the corresponding values of free space, and

$$\overline{\varepsilon} = \begin{bmatrix} \varepsilon_{xx} & \varepsilon_{xy} & \varepsilon_{xz} \\ \varepsilon_{yx} & \varepsilon_{yy} & \varepsilon_{yz} \\ \varepsilon_{zx} & \varepsilon_{zy} & \varepsilon_{zz} \end{bmatrix} \quad \overline{u} = \begin{bmatrix} \mu_{xx} & \mu_{xy} & \mu_{xz} \\ \mu_{yx} & \mu_{yy} & \mu_{yz} \\ \mu_{zx} & \mu_{zy} & \mu_{zz} \end{bmatrix} \tag{1}$$

are the relative permittivity and permeability complex tensors.

Let us consider a lossy inhomogeneous anisotropic waveguide with arbitrary cross section Ω in the x-y plane and with boundary Γ as shown in Fig. 1. This boundary is either a perfect electric conductor Γ_1, a perfect magnetic conductor Γ_2 or a combination of both. It is assumed that the cross section of the waveguide is uniform along the direction of propagation (z axis). Maxwell equations, with the electromagnetic field in the waveguide varying as $e^{(j\omega t - \gamma z)}$, take the form

$$\begin{aligned} \nabla \times \vec{E} &= -j\omega\mu_0\overline{\mu}\vec{H} \\ \nabla \times \vec{H} &= j\omega\varepsilon_0\overline{\varepsilon}\vec{E} \end{aligned} \tag{2}$$

where $\gamma = \alpha + j\beta$ is the complex propagation constant, α and β are the attenuation and phase constants, respectively, and ω is the angular frequency. The vectorial wave equation for the magnetic field, derived from Maxwell's (2) is

$$\nabla \times \overline{e}\nabla \times \vec{H} - k_0^2\overline{\mu}\vec{H} = 0 \tag{3}$$

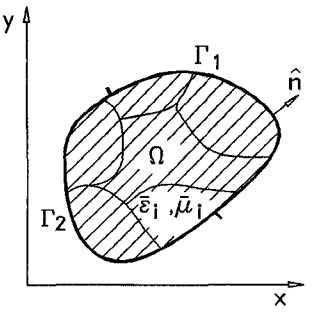

Fig. 1. General waveguide cross section.

with the boundary conditions expressed as

$$\begin{aligned} \hat{n} \times \overline{e}(\nabla \times \vec{H}) &= 0 \quad \text{on } \Gamma_1 \\ \hat{n} \times \vec{H} &= 0 \quad \text{on } \Gamma_2 \end{aligned} \tag{4}$$

where

$$\overline{e} = \overline{\varepsilon}^{-1} = \begin{bmatrix} e_{xx} & e_{xy} & e_{xz} \\ e_{yx} & e_{yy} & e_{yz} \\ e_{zx} & e_{zy} & e_{zz} \end{bmatrix}$$

k_0 is the free space wavenumber and $\hat{n}$ is a unit vector in the same plane of Ω, normal to the boundary Γ and directed outwards (Fig. 1).

Taking trial functions $\vec{H}$ and test functions $\vec{w}$ in an admissible space [17] and applying Green identities and vectorial manipulations to

$$\int_\Omega \vec{w}[\nabla \times \overline{e}\nabla \times \vec{H} - k_0^2\overline{\mu}\vec{H}]\, d\Omega = 0$$

the following expression can be derived

$$\begin{aligned} \mathfrak{B}(\vec{H}, \vec{w}) = &- \int_{\Gamma_1} \vec{w}[\hat{n} \times \overline{e}\nabla \times \vec{H}]\, d\Gamma_1 \\ &+ \int_{\Gamma_2} [\overline{e}\nabla \times \vec{H}] \cdot [\hat{n} \times \vec{w}]\, d\Gamma_2 \end{aligned} \tag{5}$$

where $\mathfrak{B}(\vec{H}, \vec{w})$ is a bilinear form. By splitting the trial functions $\vec{H}$, the test functions $\vec{w}$ and the operator ∇ into their transverse and axial parts

$$\begin{aligned} \vec{H} &= \vec{H}_t + H_z\hat{z} \\ \vec{w} &= \vec{w}_t + w_z\hat{z} \\ \nabla &= \nabla_t - \gamma\hat{z} \end{aligned}$$

where, $\nabla_t = \hat{x}\partial/\partial x + \hat{y}\partial/\partial y$, $\mathfrak{B}(\vec{H}, \vec{w})$ can be expressed as

$$\begin{aligned} \mathfrak{B}(\vec{H}, \vec{w}) = \int_\Omega [&\nabla_t \times \vec{w}_t\overline{e}'\nabla_t \times \vec{H}_t + \gamma\vec{w}_t\overline{e}'\nabla_t \times \vec{H}_t \\ &- \nabla_t w_z\overline{e}'\nabla_t \times \vec{H}_t - \gamma\nabla_t \times \vec{w}_t\overline{e}'\vec{H}_t \\ &- \gamma^2\vec{w}_t\overline{e}'\vec{H}_t + \gamma\nabla_t w_z\overline{e}'\vec{H}_t \\ &- \nabla_t \times \vec{w}_t\overline{e}'\nabla_t H_z - \gamma\vec{w}_t\overline{e}'\nabla_t H_z \\ &+ \nabla_t w_z\overline{e}'\nabla_t H_z - k_0^2\vec{w}_t\overline{\mu}\vec{H}_t - k_0^2 w_z\overline{\mu}H_z \\ &- k_0^2\vec{w}_t\overline{\mu}\hat{z}H_z - k_0^2 w_z\hat{z}\overline{\mu}H_t]\, d\Omega \end{aligned}$$

where

$$\overline{\overline{e}}' = \begin{bmatrix} e_{yy} & -e_{yx} & e_{yz} \\ -e_{xy} & e_{xx} & -e_{xz} \\ e_{zy} & -e_{zx} & e_{zz} \end{bmatrix}.$$

Assuming that homogeneous boundary conditions are imposed as

$$\hat{n} \times \vec{w} = 0 \quad \text{on } \Gamma_2$$

and natural boundary conditions as

$$\hat{n} \times \overline{\overline{e}}(\nabla \times \vec{H}) = 0 \quad \text{on } \Gamma_1$$

the equation (5) diminish to

$$\mathfrak{B}(\vec{H}, \vec{w}) = 0 \tag{6}$$

$\vec{H}$ and $\vec{w}$ are taken in the same admissible space of functions, these being smooth enough for the variational problem (6) to make sense and defined as

$$\mathcal{C} = \{\vec{v} | \hat{z} \cdot \nabla_t \times \vec{v}_t \in \mathcal{L}^2(\Omega), \quad \nabla_t v_z \in \{\mathcal{L}^2(\Omega)\}^2, \vec{v} \in \{\mathcal{L}^2(\Omega)\}^3\}$$

where $\mathcal{L}^2(\Omega)$ is a set of equivalence classes of square-integrable functions over Ω.

III. Finite Element Discretization

Let us divide the waveguide cross section into a number of triangular hybrid vector finite elements that combine edge elements of degree one for the transverse components of the magnetic field with first-order Lagrangian basis functions for the longitudinal one, as proposed in [18]. The discretized magnetic field in every element can be expressed as

$$\begin{bmatrix} \{H_p\}_e \\ \{H_q\}_e \\ \{H_z\}_e \end{bmatrix} = \begin{bmatrix} \langle 0 \rangle & \langle T_p(i,j) \rangle \\ \langle 0 \rangle & \langle T_q(i,j) \rangle \\ \langle N_i \rangle & \langle 0 \rangle \end{bmatrix} \begin{bmatrix} \{H_z\}_e \\ \{H_t\}_e \end{bmatrix}$$

where $\langle N_i \rangle$ are the first-degree Lagrange polynomials in the reference space (p, q) and

$$\vec{T}(i,j) = N_i \nabla N_j - N_j \nabla N_i = T_p(i,j)\vec{p} + T_q(i,j)\vec{q}$$

is the vectorial basis function for edge (i, j).

In order to group all the terms that including any of the factors $e_{iz}, e_{zi}, \mu_{iz}, \mu_{zi}$ with $i = x, y$, the z-component of the magnetic field is replaced by $H_z = H_z' \cdot \gamma$. By discretizing the expression in (6) and making both the trial and test functions be the same, the following quadratic eigensystem is obtained

$$(\gamma^2[M_1] + \gamma[M_2] + [M_3]) \quad \{H\} = 0. \tag{7}$$

In this eigensystem $\{H\}$ is

$$\{H\} = \begin{Bmatrix} \{H_z'\} \\ \{H_t\} \end{Bmatrix}$$

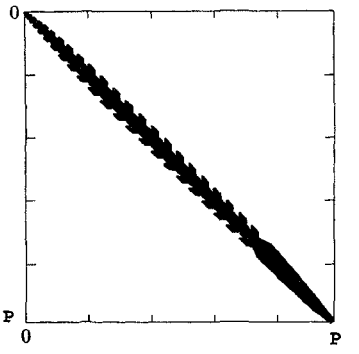

Fig. 2. Shape of the sparse matrices of order P. The terms that would be necessary to store are indicated in black. The figure corresponds to $[M_i]$ matrices for $P = N$ and $[K]$ and $[M]$ for $P = 2N$.

and the $[M_i]$ are sparse, and generally complex and neither Hermitian nor symmetrical N-by-N matrices given as

$$[M_1] = \sum_e \begin{bmatrix} [T_8] - [T_{11}] & [T_5] \\ -[T_7] & -[T_6] \end{bmatrix}$$

$$[M_2] = \sum_e \begin{bmatrix} [0] & -[T_3] - [T_{13}] \\ -[T_9] - [T_{12}] & [T_2] - [T_4] \end{bmatrix}$$

$$[M_3] = \sum_e \begin{bmatrix} [0] & [0] \\ [0] & [T_1] - [T_{10}] \end{bmatrix} \tag{8}$$

with $[T_i]$ as given in Appendix. Notice that M_3 is a singular matrix. The quadratic eigensystem (7) has been derived by taking γ as eigenvalue. A simplified generalized eigensystem form can be deduced by considering k_0^2 instead of γ as the eigenvalue. However in this paper, the formulation in (7) has been chosen in order to make the method applicable to lossless waveguides with complex modes on the one hand and to lossy ones on the other. Fig. 2 indicates the shape of the $[M_i]$ matrices in (7) when $P = N$. This was obtained by applying the aforementioned discretization method to a typical waveguide problem. The only terms that would be necessary to store are indicated in black. They show the high sparsity that is found in these matrices.

The quadratic eigenvalue problem (7) in terms of N-by-N matrices $[M_i]$, can be solved by reducing it to the standard form by means of the inversion of a matrix. This process leads to a standard eigensystem with $2N$-by-$2N$ full-matrices [10], [19].

In this paper a different approach has been followed in order to retain the sparse properties of the matrices. Let us suppose that the quadratic eigensystem with N-by-N matrices in (7) is expressed as the following equivalent generalized eigenvalue problem with $2N$-by-$2N$ matrices

$$[K]'\{X\}' - \gamma[M]'\{X\}' = 0 \tag{9}$$

where

$$[K]' = \begin{bmatrix} [0] & [I] \\ [M_3] & [M_2] \end{bmatrix} \quad [M]' = \begin{bmatrix} [I] & [0] \\ [0] & -[M_1] \end{bmatrix}$$

$$\{X\}' = \begin{Bmatrix} \{H\} \\ \{\overline{H}\} \end{Bmatrix} \quad \overline{H} = \gamma H. \tag{10}$$

It can be seen that the elements of $[M_3]$ are far from the diagonal of $[K]'$, forcing many elements of this matrix to be

stored (assuming matrix storage to be in band form). To avoid this drawback, it is advisable to convert the eigensystem to a more efficient form.

Let us suppose the equations in (9) numbered as $1, 2, \cdots, N, N+1, N+2, \cdots 2N$. A new eigensystem can be obtained by reordering these equations as $1, N+1, 2, N+2, \cdots, N, 2N$ and substituting the vector $\{X\}' = \langle x_1, x_2, \cdots, x_n, \overline{x}_1, \overline{x}_2, \cdots, \overline{x}_n \rangle$ by $\{X\} = \langle x_1, \overline{x}_1, x_2, \overline{x}_2, \cdots, x_n, \overline{x}_n \rangle$. After these manipulations the eigensystem (9) is transformed into a new equivalent generalized eigenvalue problem

$$[K]\{X\} - \gamma[M]\{X\} = 0 \tag{11}$$

where the band of the matrix $[M]$ is slightly larger than the one of $[M]'$ but where the band of the matrix $[K]$ is drastically smaller than the one of $[K]'$. Hence, only very few elements of both matrices need be stored. In Fig. 2, with $P = 2N$, the black area shows the storage requirements for the matrices $[K]$ and $[M]$ in (11), as derived from the quadratic eigensystem (7). It can be observed that the shape of the stored terms of $[K]$ and $[M]$ matrices in (11) is the same as the shape of the $[M_i]$ matrices in (7) but with a different scale. In fact, the ratio between stored terms in $[M_i]$ and $[K]$ or $[M]$ is the ratio between the size of the matrices, i.e., 4. Notice that if the $[M_i]$ matrices are hermitian or symmetrical, so are $[K]$ and $[M]$.

IV. Particular Cases

Some particular cases exist in which the quadratic eigensystem in (7) can be converted to a generalized eigenvalue problem without loss of the sparsity and without changing the size (N-by-N) of the matrices. The first, which is in accordance with many microwave and millimeter-wave devices, occurs when both $\overline{\varepsilon}$ and $\overline{\mu}$ tensors can be expressed as

$$\overline{\varepsilon} = \begin{bmatrix} \varepsilon_{xx} & \varepsilon_{xy} & 0 \\ \varepsilon_{yx} & \varepsilon_{yy} & 0 \\ 0 & 0 & \varepsilon_{zz} \end{bmatrix} \quad \overline{\mu} = \begin{bmatrix} \mu_{xx} & \mu_{xy} & 0 \\ \mu_{yx} & \mu_{yy} & 0 \\ 0 & 0 & \mu_{zz} \end{bmatrix}.$$

In this case $[T_i] = 0$, with $i = 2, 3, 4, 9, 12, 13$, and $[M_2] = 0$ because $e_{iz} = e_{zi} = \mu_{iz} = \mu_{zi} = 0$ with $i = x, y$. As a result, the quadratic eigenvalue problem in (7) is reduced to a generalized eigensystem with γ^2 as eigenvalue and N-by-N matrices.

A different situation takes place when the permeability and permittivity tensors can be expressed in either diagonal or scalar form. Then, the eigensystem in (7) is reduced to a N-by-N generalized form with symmetrical matrices.

In all the cases described above, the generalized eigensystem matrices will be complex if the $\overline{\varepsilon}$ or $\overline{\mu}$ tensors are so, and Hermitian or symmetrical if $\overline{\varepsilon}$ and $\overline{\mu}$ tensors are so. Finally, it should be pointed out that $[M_3]$ is always a singular matrix.

V. Resolution Method

The aforementioned generalized eigensystems have sparse, singular, and in general complex matrices which are neither Hermitian nor symmetrical. At present, no publicly available routine can solve this kind of eigenvalue problem efficiently. In this paper, a method based on the subspace iteration algorithm [20], [21] has been implemented to solve the eigensystem. In this algorithm a selected subset of desired eigenvalues λ_s and eigenvectors $\overline{v}_s$ are obtained. This algorithm finds an orthogonal basis in a vectorial subspace by means of an iterative process [21]. At the end of the process, the following eigensystem of projected operators is obtained

$$[k_s]\{x_x\} - \lambda_s[m_s]\{x_s\} = 0.$$

It has been found that an optimum selection for the subspace dimension is $2n$ where n is the number of desired eigensolutions. The set of eigenvectors in the original space $\overline{v}_s$ are calculated from $\{x_s\}$. This algorithm has been used with both N and $2N$ order matrices and with the sparsity of them fully utilized.

VI. Numerical Examples

In this section the proposed formulation is validated with some examples. First the shielded microstrip transmission line in Fig. 3 is considered with $A = 12.7$ mm, $d_1 = 1.27$ mm, $d_2 = 11.43$ mm, $W = 1.27$ mm, $\varepsilon_1 = 8.875$, $\mu_1 = 1$ and $t \simeq 0$. The figure shows the propagation constant of even modes versus frequency. Dark circles represent the results obtained with the proposed method. The broken, dotted, and solid lines represent the results for the dominant, higher-order, and complex modes, respectively, obtained by the spectral domain method [22]. These kinds of problems, with lossless, inhomogeneous and isotropic media, lead to solving a generalized eigenvalue problem with N-by-N real symmetrical matrices.

In the next example, a lossy anisotropic rectangular waveguide (Fig. 4) is analyzed. The permittivity is characterized by the tensor ε as shown in (12) at the bottom of the page, where $\varepsilon^0_{xx} = 11.86 - j0.8, \varepsilon^0_{yy} = 20.83 - j3.13, \varepsilon^0_{zz} = 11.86 - j0.8$, and ψ is the rotation angle as Fig. 4 shows. The figure displays the complex propagation constant versus rotation angle ψ. Dark circles represent the computed results in this work, and the solid lines the results in [10]. These kinds of lossy inhomogeneous anisotropic problems lead to solving a N-dimensional generalized eigenvalue problem with complex and symmetrical N-by-N matrices.

In the above example only dielectric losses were included. However, problems with conductor losses can be handled in the same way. Conductors with conductivity σ can be modelled as lossy media with imaginary permittivity $-j\sigma/\omega$. Moreover, external boundary conductors should be considered

$$\overline{\varepsilon} = \begin{bmatrix} \varepsilon^0_{xx} \cos^2 \psi + \varepsilon^0_{yy} \sin^2 \psi & (\varepsilon^0_{xx} - \varepsilon_{yy}) \sin \psi \cos \psi & 0 \\ (\varepsilon^0_{xx} - \varepsilon^0_{yy}) \sin \psi \cos \psi & \varepsilon^0_{xx} \sin^2 \psi + \varepsilon^0_{yy} \cos^2 \psi & 0 \\ 0 & 0 & \varepsilon^0_{zz} \end{bmatrix} \tag{12}$$

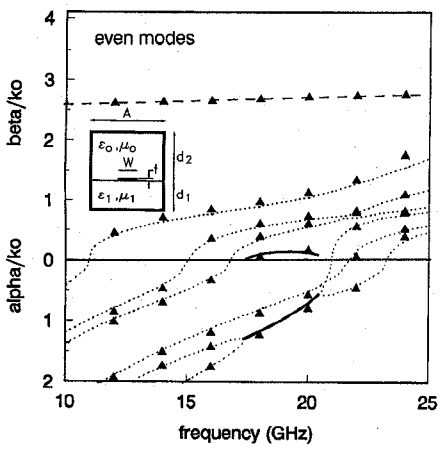

Fig. 3. Normalized propagation constant versus frequency for a shielded microstrip line. $A = 12.7$ mm, $d_1 = 1.27$ mm, $d_2 = 11.43$ mm, $W = 1.27$ mm, $\varepsilon_1 = 8.875, \mu_1 = 1$, and $t \simeq 0$. (●●●●) this work. (——, - - - -, ···) [22].

thick enough so that zero-field boundary condition could be applied in their outer side.

Fig. 5 shows the propagation characteristics at 20 GHz versus slot width for the structure depicted in the same figure. The structure consists of conductors of finite thickness and stratified media. In it, $A = 3$ mm, $d_1 = 1$ mm, $d_2 = 1$ mm, $d_3 = 3$ mm, $t = 70$ μm, $\mu_1 = 1, \varepsilon_1 = 1, \varepsilon_2 = 12.5$, the resonance line width $\Delta H = 0$, the magnetization of the ferrite $4\pi Ms = 5000$ G and the magnetic field $Ho = 500$ Oe with ferrite magnetized in the y-direction. The permeability tensor in the ferrite is defined by

$$\overline{\mu}_2 = \begin{bmatrix} 0.951 & 0 & j0.703 \\ 0 & 1 & 0 \\ -j0.703 & 0 & 0.951 \end{bmatrix}.$$

To analyze this problem, it has been necessary to solve a generalized eigenvalue problem with complex and Hermitian $2N$-by-$2N$ matrices. Dark circles show the results obtained by applying the proposed method while solid and broken lines are the results obtained with the spectral-domain approach [12]. It should be noted that forward and backward modes are not degenerate.

The next example has been included to check the proposed method in the analysis of a structure that hold non-null all the terms of a permeability tensor. In Fig. 6 the propagation properties of a line printed between ferrite superstrate and isotropic substrate are represented versus the angle ϕ of dc field. As the ferrite is magnetized with a dc field having an arbitrary direction, the terms of the permeability tensor are, in general, $\mu_{ij} \neq 0 \quad \forall i, j = x, y, z$. The frequency of analysis is 10 GHz, the angle θ of dc field is $\theta = 90°, d_1 = 0.254$ mm, $d_2 = 0.254$ mm, $W = 1.016$ mm, $\varepsilon_1 = 12.9, \mu_1 = 1, \varepsilon_2 = 12.6, \Delta H = 0, 4\pi Ms = 2750$ G and $Ho = 275$ Oe.

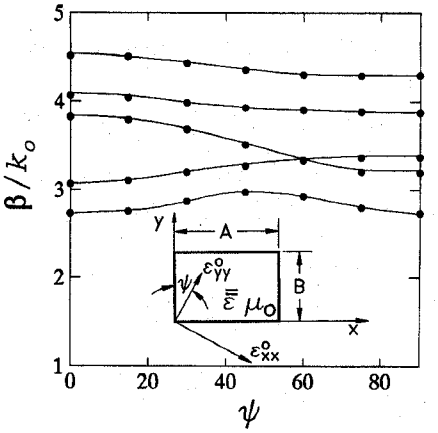

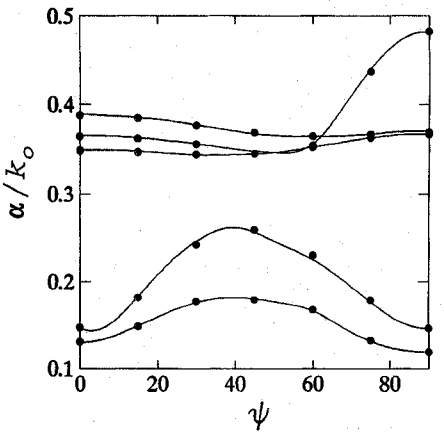

Fig. 4. Normalized propagation constant versus rotation angle (degrees) for a rectangular waveguide filled with lossy anisotropic material. $B/A = 0.4454$, $k_o A = 4.5115$. (a) Normalized phase constant. (b) Normalized attenuation constant. (●●●●) this work. (——) [10].

In this case the permeability tensor for the ferrite is expressed as in (13) shown at the bottom of the page, where μ and κ can be obtained from the expressions in [23]. The computed results are shown with dark circles in Fig. 6. They have been compared with those obtained in [13] and [23]. The solid and broken lines represent the forward and reverse solutions in [13], respectively, and the dotted and broken-dotted lines represent the solutions in [23]. It can be seen that the FEM solutions are closer to [23] than to [13]. In this case it was necessary to solve a generalized eigensystem with complex and Hermitian $2N$-by-$2N$ matrices.

In the next example, a waveguide with materials characterized by both permittivity and permeability tensors is analyzed. Fig. 7 shows the effective dielectric constant versus frequency for a shielded microstrip line printed on a simultaneously

$$\overline{\mu}_2 = \begin{bmatrix} \mu + (1-\mu)\cos^2\phi & -j\kappa\sin\phi & (1-\mu)\sin\phi\cos\phi \\ j\kappa\sin\phi & \mu & -j\kappa\cos\phi \\ (1-\mu)\sin\phi\cos\phi & j\kappa\cos\phi & \mu + (1-\mu)\sin^2\phi \end{bmatrix} \tag{13}$$

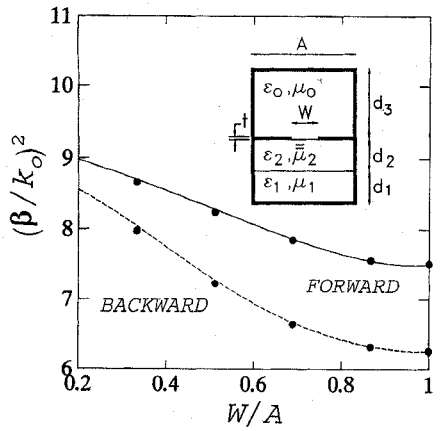

Fig. 5. Normalized propagation constant versus slot width for a finline with single-layered ferrite. $A = 3$ mm, $d_1 = 1$ mm, $d_2 = 1$ mm, $d_3 = 3$ mm, $t = 70\mu$m, $f = 20$ GHz, $\mu_1 = 1, \varepsilon_1 = 1, \varepsilon_2 = 12.5, \Delta H = 0, 4\pi Ms = 5000$ G, and $Ho = 500$ Oe.(●●●●) this work. (——, - - - -) [12].

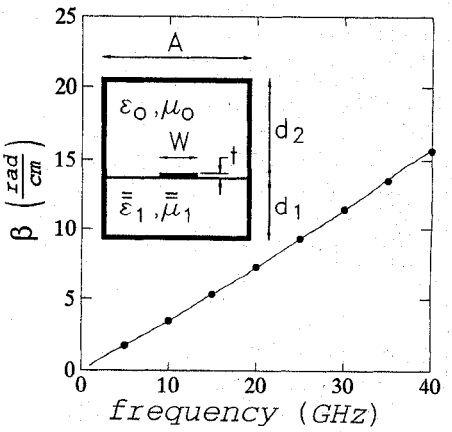

Fig. 7. Phase constant versus frequency of a microstrip line with anisotropic substrate. $d_1 = 0.5$ mm, $d_2 = 4.884$ mm, $W = 0.5$ mm, $A = 4.318$ mm, $t \simeq 0$, $\varepsilon_{xx} = 2., \varepsilon_{yy} = 2.35, \varepsilon_{zz} = 3.5, \mu_{xx} = 2.75, \mu_{yy} = 2.25, \mu_{zz} = 5.$ (●●●●) this work. (——) [14].

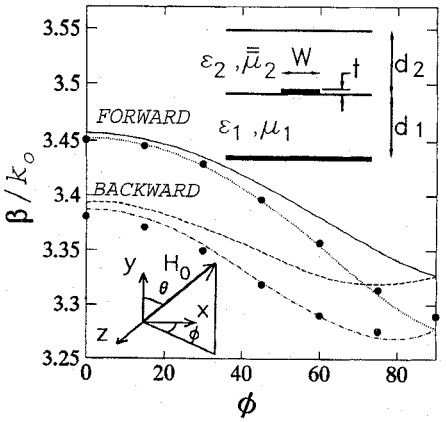

Fig. 6. Normalized propagation constant versus angle of magnetization in the x-y plane, ϕ (degrees), in a microstrip transmission line with anisotropic superstrate. $f = 10$GHz, $\theta = 90°, d_1 = 0.254$ mm, $d_2 = 0.254$ mm, $W = 1.016$ mm, $\varepsilon_1 = 12.9, \mu_1 = 1, \varepsilon_2 = 12.6, \Delta H = 0, 4\pi Ms = 2750$ G and $Ho = 275$ Oe. (●●●●) this work. (——, - - - -) [13]. ($\cdots$, — · — ·) [23].

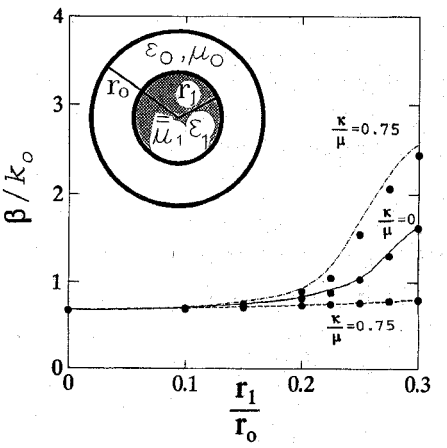

Fig. 8. Normalized phase constant for a circular waveguide with a longitudinally-magnetized concentric ferrite rod. $\varepsilon_1 = 10, k_o r_o = 2.5133$. (●●●●) this work. (——, - - - -, — · — ·) $HE_{\pm 1,1}, HE_{-1,1}, HE_{+1,1}$, respectively, in [24].

anisotropic substrate. This substrate is characterized by

$$\bar{\bar{\varepsilon}}_1 = \begin{bmatrix} 2 & 0 & 0 \\ 0 & 2.35 & 0 \\ 0 & 0 & 3.50 \end{bmatrix}$$

$$\bar{\bar{\mu}}_1 = \begin{bmatrix} 2.75 & 0 & 0 \\ 0 & 2.25 & 0 \\ 0 & 0 & 5 \end{bmatrix}.$$

The geometric data are $d_1 = 0.5$ mm, $d_2 = 4.884$ mm, $W = 0.5$ mm, $A = 4.318$ mm, and $t \simeq 0$. The results obtained by the present method are drawn with dark circles. They are compared with those in [14]. This case was analyzed by solving a generalized eigenvalue problem with real and symmetrical N-by-N matrices.

To solve a geometry with a curved boundary, a circular waveguide with a longitudinally concentric ferrite rod was analyzed. In this case the permeability is expressed as

$$\bar{\bar{\mu}}_2 = \begin{bmatrix} \mu & -j\kappa & 0 \\ j\kappa & \mu & 0 \\ 0 & 0 & 1 \end{bmatrix}.$$

Fig. 8 shows the normalized phase constant versus ratio r_1/r_o for the dominant mode with μ/κ a as parameter. The computed results obtained by the present method are printed with dark circles. Solid lines represent analytical results from [24]. This problem produces a N-dimensional generalized eigenvalue problem with complex and Hermitian matrices.

In Table I the memory requirements and CPU times for the examples analyzed herein are presented. The types of eigensystems and matrices, as well as the number of unknowns that have been utilized are also shown. These examples have been analized using a HP 9000/730.

VII. Conclusion

A new finite element formulation for solving lossy inhomogeneous anisotropic arbitrarily shaped waveguides which

TABLE I
THE MEMORY REQUIREMENTS AND CPU TIMES ON A HP 9000/730

Example	CPU time seg. per point	Memory required Mbytes	Number of unknowns	Eigensystem	Matrices
Fig.3	27.1	2.62	2356	Generalized	Real
Fig.4	25.2	1.34	1225	Generalized	Complex
Fig.5	417.5	24.3	3221	Quadratic	Complex
Fig.6	401.8	23.82	3082	Quadratic	Complex
Fig.7	45.8	4.12	2559	Generalized	Real
Fig.8	54.5	5.58	2129	Generalized	Complex

include materials with both full $[\varepsilon]$ and $[\mu]$ tensors and reentrant corners, has been described. This formulation is spurious-free and leads to a quadratic eigenvalue problem of dimension N (N = number of degrees of freedom) further reduced to a $2N$-by-$2N$ generalized form retaining the sparse properties of the matrices. In particular cases where $[\varepsilon] = [\varepsilon_{tt}] + \varepsilon_{zz}\hat{z}\hat{z}$ and $[\mu] = [\mu_{tt}] + \mu_{zz}\hat{z}\hat{z}$ the order of the matrices of the generalized eigensystem can be reduced to N. A method based on the subspace iteration algorithm was implemented in order to solve the eigensystem with the sparsity of the matrices being fully utilized. Numerical examples which illustrate the different features of the method have been solved. Results show good agreement to those reported by other authors.

APPENDIX
THE EXPLICIT FORM OF SUBMATRICES $[T_i]$

The form of submatrices of $[T_i]$ in the text are given by

$$[T_1] = \iint_e e_{zz}[A]^T[A]\,dp\,dq$$

$$[T_2] = \iint_e [T]^T[\overline{e}'_{s1}][A]\,dp\,dq$$

$$[T_3] = \iint_e [D]^T[\overline{e}'_{s1}][A]\,dp\,dq$$

$$[T_4] = \iint_e [A]^T[\overline{e}'_{s2}][T]\,dp\,dq$$

$$[T_5] = \iint_e [D]^T[\overline{e}'_{tt}][T]\,dp\,dq$$

$$[T_6] = \iint_e [T]^T[\overline{e}'_{tt}][T]\,dp\,dq$$

$$[T_7] = \iint_e [T]^T[\overline{e}'_{tt}][D]\,dp\,dq$$

$$[T_8] = \iint_e [D]^T[\overline{e}'_{tt}][D]\,dp\,dq$$

$$[T_9] = \iint_e [A]^T[\overline{e}'_{s2}][D]\,dp\,dq$$

$$[T_{10}] = \iint_e k_0^2[T]^T[\overline{\mu}_{tt}][T]\,dp\,dq$$

$$[T_{11}] = \iint_e k_0^2\mu_{zz}[N]^T[N]\,dp\,dq$$

$$[T_{12}] = \iint_e k_0^2[T]^T[\overline{\mu}_{s1}][N]\,dp\,dq$$

$$[T_{13}] = \iint_e k_0^2[N]^T[\overline{\mu}_{s2}][T]\,dp\,dq$$

where

$$[\overline{\mu}_{s1}] = \begin{Bmatrix}\mu_{xz}\\ \mu_{yz}\end{Bmatrix} \qquad [\overline{e}'_{s1}] = \begin{Bmatrix}e_{yz}\\ -e_{xz}\end{Bmatrix}$$

$$[\overline{\mu}_{s2}] = \langle \mu_{zx}\mu_{zy}\rangle \qquad [\overline{e}'_{s2}] = \langle e_{zy} - e_{zx}\rangle$$

$$[\overline{\mu}_{tt}] = \begin{bmatrix}\mu_{xx} & \mu_{xy}\\ \mu_{yx} & \mu_{yy}\end{bmatrix} \qquad [\overline{e}'_{tt}] = \begin{bmatrix}e_{yy} & -e_{yx}\\ -e_{ry} & e_{xx}\end{bmatrix}$$

$$[T] = \begin{bmatrix}\langle T_p\rangle\\ \langle T_q\rangle\end{bmatrix} \qquad [D] = \begin{bmatrix}\langle \frac{\partial N_r}{\partial p}\rangle\\ \langle \frac{\partial N_i}{\partial q}\rangle\end{bmatrix}$$

$$[N] = \langle N_i\rangle \qquad [A] = \left\langle \frac{\partial T_q}{\partial p} - \frac{\partial T_p}{\partial q}\right\rangle.$$

REFERENCES

[1] N. G. Alexopoulos, "Integrated circuit structures on anisotropic substrates," *IEEE Trans. Microwave Theory Tech.*, vol. 33, no. 10, pp. 847–851, Oct. 1985.

[2] Y. Chen and B. Beker, "The method of lines analysis of striplines with double-layered or suspended bianisotropic biaxial substrates," *IEEE Trans. Microwave Theory Tech.*, vol. 42, no. 5, pp. 917–920, May 1994.

[3] ——, "Spectral-domain analysis of open and shielded slotlines printed on various anisotropic substrates," *IEEE Trans. Microwave Theory Tech.*, vol. 41, no. 11, pp. 1872–1877, Nov. 1993.

[4] ——, "Analysis of bilateral coplanar waveguides printed on anisotropic substrates for use in monolithic MIC's," *IEEE Trans. Microwave Theory Tech.*, vol. 41, no. 9, pp. 1489–1493, Sept. 1993.

[5] Z. Cai and J. Bornemann, "Generalized spectral-domain analysis for multilayered complex media and high-Tc superconductor applications," *IEEE Trans. Microwave Theory Tech.*, vol. 40, no. 12, pp. 2251–2257, Dec. 1992.

[6] T. Q. Ho and B. Beker, "Analysis of bilateral fin-lines on anisotropic substrates," *IEEE Trans. Microwave Theory Tech.*, vol. 40, no. 2, pp. 405–409, Feb. 1992.

[7] Y. Lu and F. A. Fernández, "Vector finite element analysis of integrated optical waveguides," *IEEE Trans. Magn.*, vol. 30, no. 5, pp. 3116–3119, Sept. 1994.

[8] ——, "An efficient finite element solution of inhomogeneous anisotropic and lossy dielectric waveguides," *IEEE Trans. Microwave Theory Tech.*, vol. 41, no. 6–7, pp. 1215–1223, June–July 1993.

[9] B. M. Dillon, A. A. P. Gibson, and J. P. Webb, "Cut-off and phase constant of partially filled axially magnetized, gyromagnetic waveguides using finite elements," *IEEE Trans. Microwave Theory Tech.*, vol. 41, no. 5, pp. 803–808, May 1993.

[10] K. Hayata, K. Miura, and M. Koshiba, "Full vectorial finite element formalism for lossy anisotropic waveguides," *IEEE Trans. Microwave Theory Tech.*, vol. 37, no. 5, pp. 875–883, May 1989.

[11] I. Bardi and O. Biro, "An efficient finite-element formulation without spurious modes for anisotropic waveguides," *IEEE Trans. Microwave Theory Tech.*, vol. 39, no. 7, pp. 1133–1139, July 1991.

[12] T. Kitazawa, "Analysis of shielded striplines and finlines with finite metallization thickness containing magnetized ferrites," *IEEE Trans. Microwave Theory Tech.*, vol. 39, no. 1, pp. 70–74, Jan. 1991.

[13] I. Y. Hsia, H. Y. Yang, and N.G. Alexopoulus, "Basic properties of microstrip circuit elements on nonreciprocal substrate supertrate structures," in *Proc. IEEE MTT-S Dig.*, June 1990, pp. 665–668.

[14] T. Q. Ho and B. Beker, "Frequency dependent characteristics of shielded broadside coupled microstrip lines and anisotropic substrates," *IEEE Trans. Microwave Theory Tech.*, vol. 39, no. 6, pp. 1021–1025, June 1991.

[15] B. M. Dillon and J. P. Webb, "A comparison of formulations for the vector finite element analysis of waveguides," *IEEE Trans. Microwave Theory Tech.*, vol. 42, no. 2, pp. 308–316, Feb. 1994.

[16] J. F. Lee, "Finite element analysis of lossy dielectric waveguides," *IEEE Trans. Microwave Theory Tech.*, vol. 42, no. 6, pp. 1025–1031, June 1994.

[17] G. F. Carey and J. T. Oden, *Finite elements: A second course,* vol. 2. Englewood Cliffs, NJ: Prentice-Hall, 1983.
[18] J. F. Lee, D. K. Sun, and Z. J. Cendes, "Full-wave analysis of dielectric waveguides using tangencial vector finite elements," *IEEE Trans. Microwave Theory Tech.,* vol. 39, pp. 1262–1271, Aug. 1991.
[19] Y. Long and M. Koshiba, "Evaluation of loss factor of multilayered inhomogeneous waveguides for magnetostatic waves using efficient finite element formalism," *IEEE Trans. Microwave Theory Tech.,* vol. 37, no. 4, pp. 680–685, Apr. 1989.
[20] F. A. Fernandez, J. B. Davies, S. Shu, and Y. Lu, "Sparse matrix Eigenvalue solver for finite element solution of dielectric waveguides," *Electron. Lett.,* vol. 27, no. 20, pp. 1824–1826, Sept. 26, 1991.
[21] K. Bathe, *Finite element procedures in engineering analysis.* Englewood Cliffs, NJ: Prentice-Hall, 1982.
[22] M. S. Alam, K. Hirayama, Y. Hayashi, and M. Koshiba, "A vector finite—Element analysis of complex modes in shielded microstrip lines," *Microwave and Optical Technology Lett.,* vol. 6, no. 16, pp. 873–875, Dec. 1993.
[23] F. L. Mesa, "Estudio de las características de propagación electromagnética en líneas multiconductoras de configuración planar inmersas en medios bianisótropos estratificados," Ph.D. dissertation, Facultad de Física, Universidad de Sevilla, Sevilla, Spain, Nov. 1991.
[24] R. A. Waldron, "Electromagnetic wave propagation in cylindrical waveguides containing gyromagnetic media," *J. Brit. Instn. Radio Engnrs.,* vol. 18, pp. 597, 677, 733, 1958.

Luis Valor was born in Madrid, Spain, in 1967. He received the Ingeniero degree in 1992 and the Ph.D. degree in 1995, both from the Universidad Politécnica de Madrid, Spain.

Since 1991 he has been with the Grupo de Electromegnetismo Aplicado y Microondas at the Universidad Politécnica de Madrid with a fellowship. His current research interests include electromagnetic propagation in inhomogeneous-anisotropic waveguides structures and computer methods in electromagnetics.

Juan Zapata received the Ingeniero de Telecomunicación degree in 1970 and the Ph.D. degree in 1974, both from the Universidad Politécnica de Madrid, Spain.

Since 1970 he has been with the Grupo de Electromagnetismo Aplicado y Microondas at the Universidad Politécnica de Madrid, where he became an Assistant Professor in 1970, Associate Professor in 1975, and Professor in 1983. His current research interests are microwave active circuits and interactions of electromagnetic fields with biological tissues, computer-aided design for microwave passive circuits, and numerical methods in electromagnetism.